NMR Studies of Low-Spin Ferric Complexes of Natural Porphyrin Derivatives. 1. Effect of Peripheral Substituents on the π Electronic Asymmetry in Biscyano Complexes

Gerd N. La Mar,* David B. Viscio, Kevin M. Smith, W. S. Caughey,[1] and Michael L. Smith[1]

Contribution from the Department of Chemistry, University of California, Davis, California 95616, and Department of Biochemistry, Colorado State University, Fort Collins 80523. *Received May 30, 1978*

Abstract: The NMR spectra of a series of low-spin, biscyano ferric complexes of 2,4-disubstituted deuteroporphyrin IX have revealed that the in-plane asymmetry, as monitored by the four ring methyl proton and C^{13}, as well as meso-proton isotropic shift spread, increases dramatically as the substituents are made more electron withdrawing. Detailed analysis of the shifts for individually assigned methyls and meso H's demonstrates that the isotropic shift differences reflect primarily differences in net transferred π spin density into individual pyrroles. Since the methyl isotropic shift average remains approximately constant with substituent, the effect of the 2,4 disubstitution is to cause a rearrangement of the delocalized spin among the four pyrroles such that ring I has the least and ring IV has the most spin density. Analysis of the shift pattern in mono- and disubstituted complexes suggests that the perturbing influences at any one methyl due to the 2 and 4 substituents are approximately additive. When a single electron-withdrawing substituent is introduced at the 4 position, the assigned methyl shift pattern closely resembles that observed for sperm whale metmyoglobin cyanide. Comparison of shift patterns in models and low-spin hemoproteins indicates that heme–apoprotein peripheral contacts most likely induce the characteristic asymmetry in the protein, and suggest that even highly localized perturbations in a protein should be reflected in shift changes at all heme methyls, as had been observed upon intercalating xenon into metmyoglobin cyanide.

Introduction

^{1}H NMR has played a central role in characterizing the electronic structure of paramagnetic porphyrins[2] and hemoproteins.[3,4] Although it is now known that the porphyrin paramagnetic shift patterns for each oxidation/spin state differ characteristically in model compounds[2,5-7] and proteins,[3,4,8-10] in that the apparent in-plane asymmetry, as indexed by the spread of the isotropic shifts for the four ring methyls in protoporphyrin, is always much larger in the protein environment, little is known as to what physical interactions[11] can give rise to these shift differences and how to interpret them. The majority of the work on qualitative characterization of this in-plane asymmetry has been carried out on the low-spin ferric systems,[3-5,8,12,13] which will also be the subject of our present study.

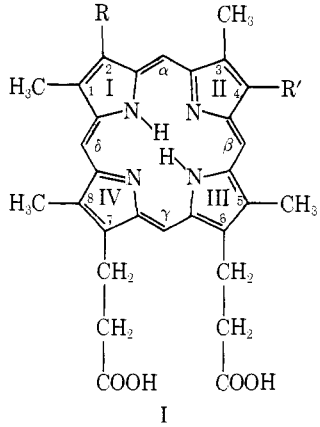

I

We report here on a series of studies aimed at establishing that systematic peripheral perturbations on a porphyrin in the form of variable-strength electron-withdrawing substituents are capable of inducing large in-plane asymmetry in low-spin ferric complexes, and that under proper control can completely mimic the protein environment.[8] In the first of this set of three reports we wish to demonstrate that this asymmetry in the porphyrin methyl isotropic shifts reflects an asymmetric distribution of the unpaired spin among the four pyrrole rings.[14] The second part of this study will illustrate[15] that intermolecular paramagnetic dipolar relaxation can be used to determine the solution structure of low-spin ferric porphyrin dimers,[16] and that the nature of the interaction within the dimer suggests π complex formation between two rhombically asymmetric π systems. In the last part of this study, we show[17] that the thermodynamics of the dimerization and stereospecificity of the dimer interaction are controlled by this in-plane π asymmetry, providing evidence that the in-plane asymmetry is reflected in the whole π system, not only in the spin-containing orbital.

Our subject compounds are the biscyano, low-spin ferric complexes of a series of derivatives of deuteroporphyrin (I), substituted at the 2 and/or 4 positions. Although such porphyrins are usually treated as possessing essentially fourfold symmetry, with peripheral substituents exerting only a negligible perturbation on the system, only the mesoporphyrin complex (R = R′ = ethyl) should approach fourfold symmetry, since the 2,4 substituents are alkyls (ethyls), as are the four methyl groups and the two propionic acid side chains common to all derivatives of interest. All other 2,4-R_2 can be arranged in order of increasing electron-withdrawing power, i.e., ethyl < hydrogen ≲ vinyl < bromine < sulfonate < acetyl < formyl < cyanide,[18,19] which will induce increasing distortions from fourfold symmetry. In order to establish the effects of variable 2,4-R_2 on the electronic structure, we wish to monitor the methyl environments in each pyrrole. The ^{1}H NMR spectra of a few of our model compounds have been reported but not assigned.[20-22] The individual methyls of both the protoporphyrin (R = vinyl) model complex[12] and sperm whale cyanometmyoglobin[8] have been reported.

Principles

The characterization of the in-plane asymmetry in paramagnetic porphyrins using NMR involves a detailed analysis of the origin of the isotropic shifts in terms of possible magnetic anisotropy and transferred unpaired spin density. The isotropic

0002-7863/78/1500-8085$01.00/0

shift for a nucleus in a complex or protein is given by

$$(\Delta H/H)_{iso} = (\Delta H/H)_{con} + (\Delta H/H)_{dip} \quad (1)$$

where the contact shift[23] is

$$(\Delta H/H)_{con} = -A\frac{g\beta S(S+1)}{(\gamma k\pi)3kT} \quad (2)$$

and the dipolar shift[23] is represented by

$$(\Delta H/H)_{dip} = 1/3N\left\{\left[\chi_z - \frac{1}{2}(\chi_x + \chi_y)\right]\frac{(3\cos^2\theta - 1)}{r^3} + \frac{3}{2}(\chi_x - \chi_y)\frac{\sin^2\theta\cos 2\Omega}{r^3}\right\} \quad (3)$$

where A is the Fermi contact coupling, χ_x, χ_y, χ_z are the principal components of the susceptibility tensor, θ is the angle between the metal-nucleus vector and the z axis, r is the length of this vector, and Ω is the angle between the projection of r on the xy plane and the x axis.

In-plane asymmetry can arise from either differences in A (transferred spin to individual pyrroles) or rhombic magnetic anisotropy (i.e., the second term in eq 3). Since low-spin ferric systems are known to be magnetically anisotropic, both cases must be considered.

Previous analyses,[6,20,24] of low-spin ferric model complexes have shown that the pyrrole substituents reflect spin density within the occupied 3e π orbital on the porphyrin, as evidenced by upfield protons and downfield methyl contact shifts. The methyl proton coupling constant and the pyrrole carbon π spin density are related by[25]

$$A^{H}_{CH_3} = Q^{H}_{CCH_3}\rho_C \quad (4)$$

$Q^{H}_{CCH_3}$ is a variable positive parameter because the extent of hyperconjugative coupling depends on the electronic structure of the π subunit. In order to distinguish between changes in $Q^{H}_{CCH_3}$ and ρ_c, it is often desirable to look at the ^{13}C signal of the methyl group, for which we have[26]

$$A^{C}_{CH_3} = Q^{C}_{CCH_3}\rho_C \quad (5)$$

but where $Q^{C}_{CCH_3}$ can now be considered a negative constant much in the same way as that for a directly bonded proton. Hence changes in $A^{C}_{CCH_3}$ necessarily reflect changes only in ρ_C.

Some information on the origin of the in-plane asymmetry can also be derived from qualitative considerations of the relaxation data. The methyl proton line width, $(1/\pi T_2)$, in the fast-motion limit ($\omega_s^2\tau_s^2 \ll 1$) is given by[27]

$$(\pi T_2)^{-1} = [Dr^{-6} + C(A/\hbar)^2]\tau_S \quad (6)$$

where $D = 2g^2\beta^2\gamma^2S(S+1)/3$, $C = 2S(S+1)/3$, and τ_S is the electron relaxation time. The first term is due to dipolar relaxation, while the latter term represents scalar or contact relaxation. If $r(r^{-6})$ for a given set of methyls is constant, sizable differences in overall paramagnetic relaxation rates must reflect primarily variations in $(A/\hbar)^2$ for the methyls.

Experimental Section

Protoporphyrin IX iron(III) chloride was used as purchased from Sigma. All other 2,4-disubstituted deuteroporphyrin IX iron(III) chloride complexes were synthesized using standard procedures. Deuteroporphyrin IX iron(III) chloride, mesoporphyrin IX iron(III) chloride, 2,4-dibromodeuteroporphyrin IX iron(III) chloride, and the three acetyl-substituted derivatives, 2,4-diacetyl-, 2-acetyl- and 4-acetyldeuteroporphyrin IX iron(III) chloride, were synthesized by the methods of Falk,[28] Baker et al.,[29] Fischer,[30] and Caughey et al.,[31] respectively. The dimethyl ester derivatives of the above complexes were synthesized by the method of Caughey et al.[31] The dimethyl esters were purified by chromatographing on Fisher A-540 alumina deactivated with 10% w/w water. The dimethyl esters were eluted with 3:1 chloroform–benzene and evaporated to dryness yielding the μ-oxo dimer derivatives. The μ-oxo dimers were converted to the chloride complexes by dissolving 1 g in 50 mL of chloroform, shaking with 30 mL of 0.1 M HCl, and evaporating to dryness.

The 2,4-diformyl-, 2,4-dicyano-, 2-formyl-4-vinyl-, and 2-vinyl-4-formyldeuteroporphyrin IX dimethyl ester iron(III) chloride complexes were synthesized by inserting iron [32] into the porphyrin ligands synthesized by the methods of Sparatore and Mauzerall,[33] Caughey et al.,[31] and Kenner et al.,[34] respectively. The 2-formyl-4-vinyl- and 2-vinyl-4-formyldeuteroporphyrin IX iron(III) chloride complexes were made by first deesterifying the ligands by the method of Kenner et al.[34] followed by insertion of iron.[32] 2,4-Disulfonatedeuteroporphyrin IX iron(III) chloride was a gift from H. Goff.

The regioselectively deuterated protoporphyrin IX dimethyl ester iron(III) chloride complexes were prepared by inserting iron[32] into deuterated protoporphyrin IX dimethyl ester ligands synthesized by the methods of Cavaleiro et al.[35] and Evans et al.[14] All other deuterated 2,4-disubstituted deuteroporphyrin IX dimethyl ester iron(III) chloride complexes were synthesized by the previously described procedures. All dimethyl esters were deesterified by the method of Falk.[36] Purity of all complexes was verified by the ^1H NMR of the biscyano derivatives.

The low-spin biscyano complexes studied were prepared by dissolving the appropriate porphyrin iron(III) chloride with at least 4:1 potassium cyanide in $C^2H_3O^2H$ in the NMR sample tube. Sample concentration ranged from 0.001 to 0.05 M. For simplicity, all the biscyano complexes will be named as derivatives of deuteroporphyrin IX iron(III) dicyanide (2,4-H_2DC) and will be abbreviated 2-R,4-R′-DC. The dimethyl ester complexes will be 2-R,4-R′-DEC, where R, R′ = E, ethyl; H, hydrogen; V, vinyl; B, bromine; A, acetyl; S, sulfonate; F, formyl; and C, cyanide.[37]

NMR spectra were obtained on a JEOL JNM-PS-100 pulsed FT NMR spectrometer operating at 99.5 MHz for proton and 25.0 MHz for carbon-13. The spectrometer was equipped with a JEOL EC-100 data system. Me_4Si was used as an internal standard and, unless otherwise stated, the temperature was 25 °C. For ^1H NMR spectra, up to 1000 transients were accumulated using ca. 20 μs 90° pulses with 8K data points over a 4-kHz bandwidth. For ^{13}C NMR spectra, up to 200 000 transients were accumulated using ca. 20-μs pulses with 8K data points over a 10-kHz bandwidth. Carbon atoms bound directly to protons could be identified from the residual ^{13}C–^1H spin–spin coupling in a CW off-resonance proton double irradiation experiment.

Results

^1H NMR traces of the methyl region for the complexes 2,4-R_2DC in $C^2H_3O^2H$, with R = ethyl, hydrogen, vinyl, bromine, and acetyl, are illustrated in Figure 1. The NMR spectra were concentration independent at 25 °C indicating the absence of aggregation of the complexes. The four methyls in each of these complexes, as well as their dimethyl ester complexes, 2,4-R_2DEC, were unambiguously assigned by specific deuteration. The isotropic shifts for these five free-acid complexes in Figure 1, as well as those of three complexes for which specific methyl assignments were not made, R = sulfonate, formyl, and cyanide, are listed in Table I.

The pattern of the methyl assignments in free acid and dimethyl ester complexes were found to be the same with the exception of 2,4-R_2 = ethyl (vide infra). The position of the assigned individual methyls differed only slightly, but in a highly characteristic manner, i.e., the differences in positions in the free acid and esterified forms differed by a fixed amount in *all* complexes. On going from the free acid (R_2DC) to ester (R_2DEC), these systematic methyl shifts were found to be 1-CH_3, 0.70 ± 0.15 ppm downfield; 3-CH_3, 0.11 ± 0.10 ppm downfield; 5-CH_3, 1.20 ± 0.28 ppm upfield; 8-CH_3, 1.34 ± 0.11 ppm upfield. Since the order of observed shifts for methyls is 1, 3, 5, 8, going downfield, the effect of esterification is to *decrease* the net spread of the four methyls in all cases but 2,4-R_2 = ethyl. In the latter case, esterification reverses the relative positions of the 1,3-CH_3 and 5,8-CH_3 pairs (vide infra).

Table I. Proton Isotropic Shifts of 2,4-R_2DC[a]

position		R = E	H	V	B	S	A	F[b]	C[b]
ring methyl	1	−12.63	−9.99	−9.31	−6.52	−3.95	−0.72	+0.10	+0.82
	3	−12.10	−11.64	−10.55	−9.55	−8.63	−7.60	−8.33	−8.03
	5	−12.98	−12.72	−13.95	−16.57	−14.58	−13.84	−12.80	−15.27
	8	−12.98	−15.26	−14.30	−17.00	−16.59	−18.14	−19.30	−21.72
	spread	0.35	5.27	4.99	10.48	12.64	17.42	19.4	22.54
	av	−12.67	−12.40	−12.03	−12.41	−10.94	−10.08	−10.08	−11.05
meso	α	9.09	9.21	10.74	11.90	13.37	17.70	16.23	14.96
	β	8.82	9.21	9.46	10.37	12.10	13.21	12.69	10.35
	δ	8.40	8.61	9.97	9.83	7.98	10.59	9.65	10.08
	γ	6.69	7.26	7.39	7.30	*c*	8.46	8.25	*c*
6,7α-CH_2		−3.45	−4.02, −2.66	−3.60, −3.17	−2.89, −2.62	−4.41, −2.22	−4.76, −2.60	−3.79, −1.60	−2.13, −1.42
6,7β-CH_2		2.62	2.63	2.58	2.98	1.63, 2.14	1.98, 2.46	2.36, 2.58	2.12, 2.56
2-R		−3.10[d], 1.55[e]	24.54	−4.60[f], 7.42[g], 8.04[h]			0.88	*c*	
4-R		−2.82[d], 1.46[e]	24.82	−3.97[f], 7.17[g], 7.86[h]			0.88	*c*	

[a] Shifts in parts per million ± 0.01 ppm at 25 °C in $C^2H_3O^2H$, referenced to the following diamagnetic Zn derivatives' chemical shifts: δCH_3 −3.6, $\delta\alpha$-CH_2 −4.5, $\delta\beta$-CH_2 −3.40, $\delta_{meso\text{-}H}$ −10.50 ppm; R = E, $\delta_{\alpha CH_2}$ −4.20, $\delta_{\beta\text{-}CH_3}$ −1.9; R = H, δ_H −9.40; R = V, $\delta_{\alpha\text{-}CH}$ −8.60, $\delta_{\beta CH_2}$ −6.30; R = A, δCH_3 −3.25 ppm; downfield shifts are negative. [b] Dimethyl ester derivatives. [c] Not resolved. [d] 2,4-α-CH_2. [e] 2,4-β-CH_3. [f] α-Vinyl-H. [g] Trans-β-vinyl-H. [h] Cis-β-vinyl-H.

The absence of specifically deuterated meso H's necessitated the use of the indirect method of Brassington et al.,[38] where Mn^{2+} is added to the methanol solutions of the complex. Figure 2 exhibits the effect of this added Mn^{2+} on the line widths of the resonances of B_2DC. The Mn^{2+} coordinates at the propionic acids, probably as a chelate, and induces dipolar relaxation in heme substituents $\propto r^{-6}$. As depicted in Figure 3, the position of the Mn^{2+} predicts the relative methyl broadening.[27,38] The observation of the relative Mn^{2+}-induced methyl broadening pattern confirms the position of the metal ion. The relative rates of meso-H broadening in Figure 3 provide partial assignments in this case, as well as for all other free acid complexes. The isotropic shifts for all heme substituents in 2,4-R_2DC are listed in Table I.

The proton traces of the spirographis complex (2-F,4-V-DC) and isospirographis (2-V,4-F-DC) complexes are given in A of Figures 4 and 5 respectively. The former porphyrin is the natural prosthetic group of erythrocruorin.[39] The lack of deuterium labels necessitated methyl assignments using the Mn^{2+} method.[38] Trace B in each of Figures 4 and 5 illustrates the effect of added Mn^{2+} on methyl line widths. Although the 1-CH_3 and 3-CH_3 can be readily assigned, the 5-CH_3/8-CH_3 pair of signals cannot be differentiated by this method. The porphyrin methyls in the pair of complexes, 2-A-DC and 4-A-DC, were assigned using methyl deuteration as described elsewhere.[40] The isotropic shifts for the four complexes, 2-R,4-R′DC (R ≠ R′), are listed in Table II.

The proton noise-decoupled and off-resonance decoupled ^{13}C NMR spectra of each of B_2DC and A_2DC are shown in A, B, C and D, respectively, of Figure 6. The multiplet patterns and residual splittings, together with the specifically assigned methyl groups and meso H's (Table I), yield directly the methyl and meso carbon specific assignments listed in Table III.

The tabulated methyl and meso-H shifts in Table I clearly show that the spread of the four heme methyls and meso-H's resonances in R_2DC increase monotonically with the electron-withdrawing power of R. The complex with R = ethyl, anticipated to be the most symmetric, reveals essentially identical environments for the four methyls. The systematic

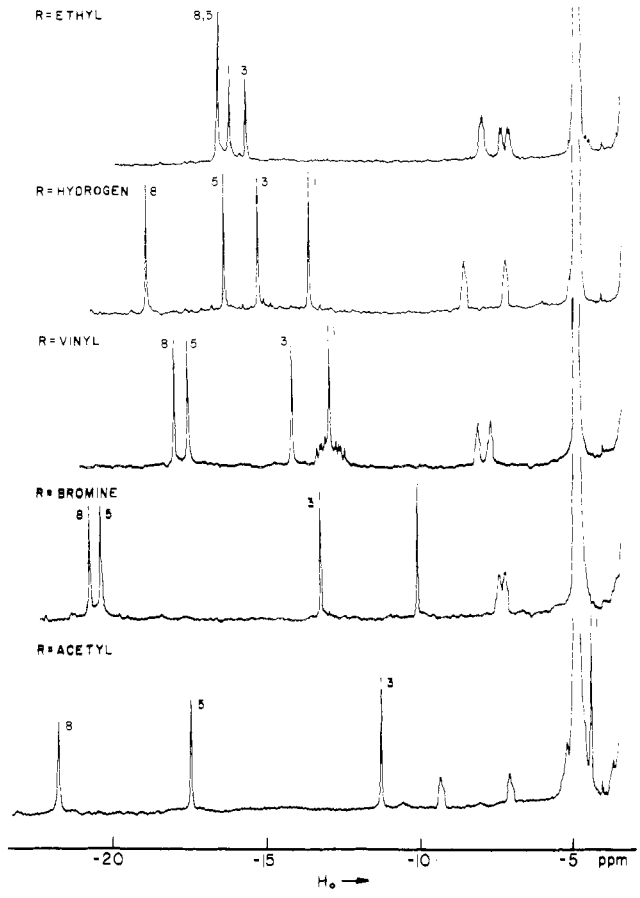

Figure 1. ^1H NMR spectra of the methyl regions of 2,4-R_2DC in $C^2H_3O^2H$ at 25 °C for R = ethyl, hydrogen, vinyl, bromine, and acetyl. The methyls were assigned by ^2H substitution.

effect of 2,4-R_2 is to move 1-CH_3 and 3-CH_3 further upfield, with the former always exhibiting the smallest shift, while 5-CH_3 and 8-CH_3 move downfield, with the latter always showing the largest shift. The data in Table II reveal that the

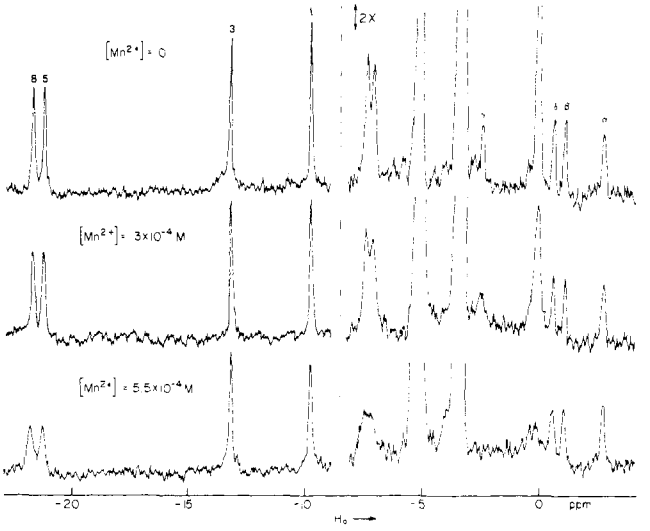

Figure 2. ^{1}H NMR spectra of 0.01 M 2,4-B_2DC in $C^2H_3O^2H$ at 10 °C showing effect of Mn(II) concentration on line widths.[38]

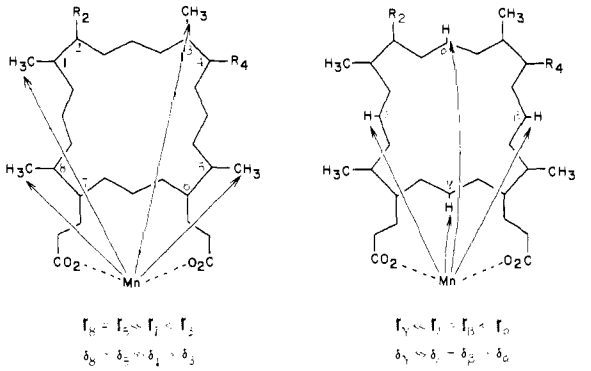

Figure 3. Relative distances of porphyrin substituents from Mn^{2+} and the relative line broadening.

trend in methyl shifts when R ≠ R′ is more complex (vide infra). The pattern in ^{13}C isotropic shifts (Table III) parallels that of the protons, with the spread of the shifts increasing as 2,4-R_2 becomes more electron withdrawing; the trend in increasing upfield methyl ^{13}C isotropic shifts is 1 < 3 < 5 < 8. The meso carbon shifts similarly spread out with R.

Discussion

Analysis of Isotropic Shifts. First we must differentiate between dominant contact and dipolar contributions to the increasing methyl proton (or meso H) shift spread as 2,4-R_2 is made more electron withdrawing. Axial anisotropy (first term in eq 3) can be eliminated since it affects all four methyls (or meso H) in the identical manner. Moreover, the ESR g values of the bisimidazole complexes[41,42] of the same series of porphyrins are essentially invariant with R, even though the heme methyl shift spread increases similarly with R. Earlier analyses[43] of the axial anisotropy suggested a 1-4-ppm upfield dipolar contribution at each methyl in methanol solution, which is probably the same for all substituents.

In-plane or rhombic magnetic anisotropy is found in the liquid-helium temperature ESR spectra of all low-spin ferric porphyrins, even fourfold symmetric complexes.[3,24,42] Rhombic magnetic anisotropy or dipolar shifts (second term in eq 3), however, as the prime source of the shift spread with 2,4-R_2 can be conclusively ruled out based on several observations. The second term in eq 3 imposes[23] certain symmetry relationships on the rhombic dipolar shift for the various methyls (or meso H's), namely, that the 1-CH_3 and 5-CH_3 (or α-H, γ-H), related by 180° rotation, must exhibit identical shifts owing to the cos 2Ω term, and that 1-CH_3 and 3-CH_3, related by 90° rotation, must have equal shifts in opposite direction. The data in Table I clearly show that 1-CH_3 and 5-CH_3 (or α-H and γ-H) move in opposite direction, while 1-CH_3 and

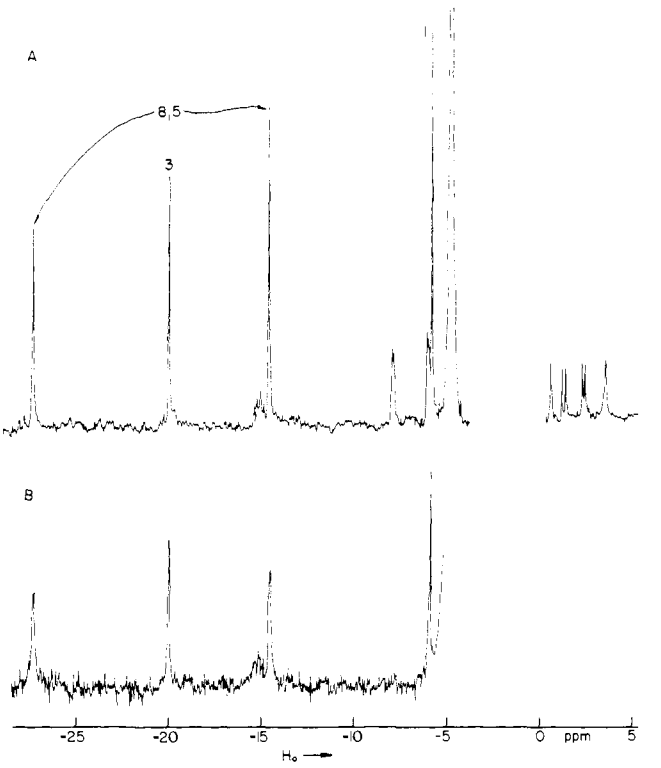

Figure 4. ^{1}H NMR spectra of 2-F, 4-V-DC in $C^2H_3O^2H$ at 25 °C showing methyl assignments by Mn(II) broadening:[38] A, [Mn(II)] = 0; B. [Mn(II)] = 6 × 10^{-4} M.

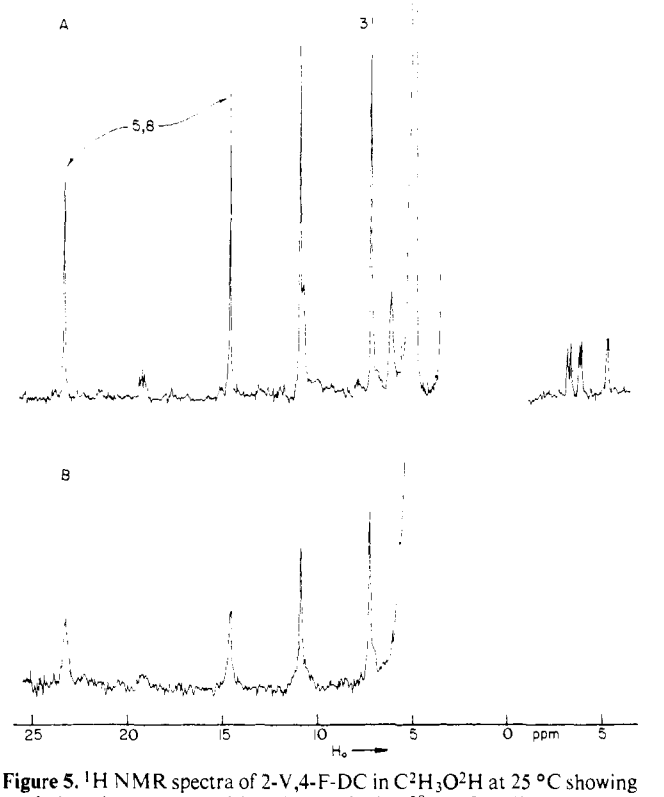

Figure 5. ^{1}H NMR spectra of 2-V,4-F-DC in $C^2H_3O^2H$ at 25 °C showing methyl assignments by Mn(II) broadening:[38] A, [Mn(II)] = 0; B. [Mn(II)] = 6 × 10^{-4} M.

Table II. Proton Isotropic Shifts for 2-R,4-R′-DC[a]

position		R = A R′ = H	H A	F V	V F	sperm whale metmyoglobin cyanide[b]
ring methyls	1	−0.98	−10.13	−2.26	−7.12	−14.6
	3	−18.58	−3.40	−16.23	−3.53	−1.4
	5	−9.48	−19.17	(−11.02, −23.57)	(−19.55, −10.96)	−23.3
	8	−24.15	−10.50			−9.6
	av	−13.30	−10.80	−13.27	−10.29	−12.2
α,β,δ,γ meso-H		13.10	14.44	13.88	15.80	
		9.58	*c*	10.98	*c*	
		c	*c*	*c*	*c*	
		c	*c*	*c*	*c*	
6,7-α-CH_2		(−4.04, −1.40)	(−6.72, −0.86)	(−3.42, −1.68)	(−6.22, −1.58)	
6,7-β-CH_2		*c*	*c*	*c*	*c*	
2-R		0.88	28.22	*c*	−10.44[d] 9.54[e] 10.14[f]	
4-R′		24.98	0.88	−6.42[d] 7.45[e] 8.54[f]	*c*	

[a] Shifts in parts per million ± 0.01 ppm at 25 °C in $C^2H_3O^2H$ referenced to the same diamagnetic shifts as in Table I. [b] See ref 8 and 9. [c] Not resolved. [d] α-Vinyl-H. [e] Trans-β-vinyl-H. [f] Cis-β-vinyl-H.

3-CH_3 move in the same directions as the spread of the resonances increases. Hence the rhombic anisotropy cannot be the major cause for the characteristic methyl or meso-H spread.

Direct support for sizable differences in contact contributions to the different methyls can be obtained from qualitative consideration of the line widths. The traces in Figure 1 clearly show that, as the methyl shift spread increases, the four methyls tend to exhibit increasingly different line widths, with the farthest upfield peak being the narrowest (1-CH_3) and the extreme downfield peak being the broadest (8-CH_3). Since the dipolar term in eq 6 contributes identically (same r^{-6}) to each methyl line width, the difference must arise from differential contact or scalar relaxation.[27] Since it is known that the π contact contribution to all methyl peaks is downfield,[5,6,20,24] increasing downfield contact shifts $(A/\hbar)^2$ should yield broader lines, as observed. The lifting of the ground-state orbital degeneracy by a rhombic perturbation[5] can be eliminated since the calculated shift pattern does not agree with the observed results.

Hence we can conclude that the change in the spread of the four methyl shifts with 2,4-R_2 reflects primarily increases in the contact shifts of 5-CH_3 and 8-CH_3, with the latter the largest, while the contact shift for 1-CH_3 and 3-CH_3 decrease, being smallest for the former. In E_2DC, which is closest to being fourfold symmetric, the methyl shifts are essentially identical, while for A_2DC, which produces the largest distortion for the complexes with assigned methyls, the spread is the largest. Although it was not practical to label the three complexes R_2DC with R = sulfonate, formyl, and cyanide, it is clear that we expect the same order in methyl assignments with the most electron-withdrawing cyanide yielding the largest asymmetry,[46] as shown in Table I.

In-Plane Electronic Asymmetry. The contact contributions to the pyrrole substituent shifts have been shown to be dominated by spin transfer into a filled 3e π molecular orbital[5,6,24] (upfield proton and downfield methyl shifts), so that the different contact shifts in Table I must reflect significant differences in the methyl coupling constant, A (eq 2), for the four pyrroles. These couplings are related to the aromatic carbon spin density, ρ_C, via eq 4. Since $Q^H_{CCH_3}$ is known to vary (+5 to +120 MHz),[25] depending on the local electronic environment, and our in-plane asymmetry is indicative of different π electron distributions, variation in either $Q^H_{CCH_3}$ or ρ_C could cause the observed changes in $A^H_{CH_3}$. However, as shown by the ^{13}C data in Table III, the methyl carbon contact shift spreads parallel the methyl proton contact shift spreads, and since $A^C_{CH_3}$ is related to ρ_C via a true constant (eq 5), a change in both methyl proton and carbon contact shift spreads must reflect differences in the extent of spin transfer, ρ_C, into individual pyrroles. Thus the order of increasing spin delocalization to the four pyrroles is I < II < III < IV, in all compounds with nonalkyl 2,4-R_2, with the spread increasing as R becomes more electron withdrawing.[45]

We note in Table I that the average methyl isotropic shifts are essentially independent of 2,4-R_2. Since we can assume that the 2,4-R_2 does not significantly alter the axial anisotropy, this

Table III. ^{13}C Isotropic Shifts of 2,4-R_2DC[a]

position		R = H	V	B	A
ring methyls	1	(38.6[b], 42.3, 46.2, 50.7)	(39.4[b], 41.6, 47.9, 48.7)	34.1	18.3
	3			40.9	33.3
	5			(57.0, 57.5)	46.2
	8			48.7	53.0
	spread	12.1	9.3	13.3	19.4
meso-C	α	(24.7, 22.6)	16.8	12.8	−49.8
	β	*c*	(27.2, 34.2)	(42.0, 44.3)	(−15.7[d], 28.6[e])
	δ	*c*	46.8	73.0	42.0
	γ				
6,7-α-CH_2		(41.5, 35.8)	(39.6, 38.1)	(40.6, 41.7)	(41.0[f], 31.9[g])
6,7-β-CH_2		(−52.7, −61.9)	(−56.3, −58.6)	(−55.8, −57.4)	(−49.6, −65.1)
R		32.1[h] 22.1	(62.5, 60.7)[i] (−44.6, −46.3)[j]		3.0[k] 3.5

[a] Shifts in parts per million ± 0.1 ppm at 25 °C referenced to diamagnetic derivatives from ref 21 and W. S. Caughey and D. Doddrell, *J. Am. Chem. Soc.*, **94**, 2510–2512 (1972). [b] Data taken from ref 21. [c] Not observed. [d] Coupled to meso-H at 13.21 ppm. [e] Coupled to meso-H at 10.59 ppm. [f] Coupled to α-CH_2 at −4.76 ppm. [g] Coupled to α-CH_2 at −2.60 ppm. [h] 2,4-Pyrrole carbons. [i] α-Vinyl carbons. [j] β-Vinyl carbons. [k] β-Acetyl CH_3.

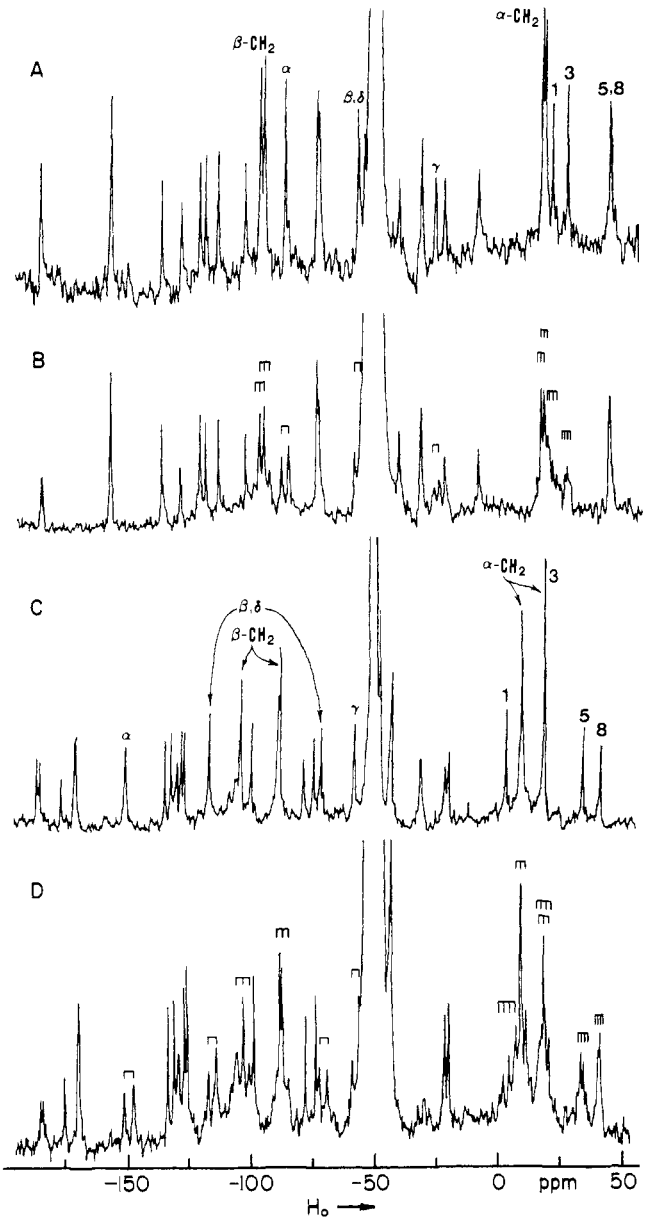

Figure 6. ^{13}C NMR spectra of 2,4-B_2DC and 2,4-A_2DC in $C^2H_3O^2H$ at 25 °C: A, 2,4-B_2DC, proton noise decoupled; B, 2,4-B_2DC, off-resonance decoupled at ca. 23 ppm downfield from Me_4Si; C, 2,4-A_2DC, proton noise decoupled; D, 2,4-A_2DC, off-resonance decoupled at ca. 26 ppm downfield from Me_4Si.

means the *net* spin transfer to the four pyrroles is approximately constant, with the result that the increasing spread of the methyl contact shifts with 2,4-R_2 must be interpreted as reflecting primarily a *redistribution* of the delocalized spin among the four pyrroles. Thus pyrroles I and II receive less spin than pyrroles III and IV in all 2,4-R_2DC, except for R = ethyl, in which the four pyrroles are nearly equivalent.

Although the π electron asymmetry induced by R with electron-withdrawing substituents provides direct information on only the unpaired spin-containing orbital, it is suggestive of an overall π cloud asymmetry. Based on the data on the contact shift this suggests that pyrroles I and II lose π electron density at the expense of pyrroles III and IV. Our inability to make a quantitative separation of axial dipolar and contact shifts prevents us from obtaining quantitative estimates of the difference in extent of spin transfer to the individual pyrroles.[46]

Inasmuch as porphyrin π clouds are often involved in π-π donor/acceptor interactions with organic aromatic molecules[47] or other porphyrins,[15,48] this suggests the possibility that the four pyrroles should differ noticeably in their relative tendencies to act as π donors and/or acceptors. Electron-deficient pyrroles I and II would appear to be better candidates as π acceptors, while pyrroles III and IV should act as better π donors. These suggestions are supported both by the unusual structures of the solution π complex dimers of R_2DC[15,16] as well as the effect of variable R on the thermodynamics of this dimerization,[17] as will be discussed in parts 2 and 3 of this study.

Table IV. Average Methyl Isotropic Shifts for Pairs of Complexes[a]

complexes	average methyl shift 8	5	3	1
2-A-DC and 4-A-DC	−17.3	−14.2	−10.5	−5.6
2,4-A_2DC and 2,4-H_2DC	−16.7	−13.3	−9.6	−5.4
2-F,4-V-DC and 2-V,4-F-DC	−17.3	−15.3	−9.9	−4.7
2,4-H_2DC and 2,4-F_2DC[b]	−17.3	−14.0	−9.4	−4.6

[a] Shift in parts per million at 25 °C in $C^2H_3O^2H$ taken from Table I. [b] See ref 49.

Effects of Multiple Perturbations. Assignment of the heme methyls[40] in 2-A-DC and 4-A-DC demonstrates that substitution at only one of the two possible positions significantly alters the simple pattern of increasing downfield shifts, $1 < 3 < 5 < 8$, as observed in all 2,4-R_2DC. Furthermore, 4-A-DC exhibits a larger methyl shift spread than 2,4-A_2DC, suggesting that substitution at both positions causes partial cancellation of effects at certain methyls. Thus the average of the shifts for individual methyl peaks in 2-A-DC and 4-A-DC is essentially identical with that of the average for the same methyls in A_2DC and H_2DC, as shown in Table IV. Comparison of 2-F,4-V-DC with 2-A-DC and 2-V,4-F-DC with 4-A-DC (Table III) reveals that they are pairwise the same as far as the assigned 1-CH_3, 3-CH_3, and 5,8-CH_3 pair are concerned. It is thus reasonable to assume that the relative assignments for 5-CH_3 and 8-CH_3 determined for 2-A-DC and 4-A-DC are valid for 2-F,4-V-DC and 2-V,4-F-DC, respectively. This is not surprising since the electron-withdrawing power of a vinyl is quite similar to that of a proton, as is that of a formyl and acetyl group. Under those conditions, the average of individual methyl shifts in these pairs of complexes is essentially identical with the average of V_2DC and F_2DC, as also shown in Table IV. These results strongly suggest that the influence on individual heme methyls due to substitution at the 2 and 4 positions exhibits additive character.

Further support for the additive nature of substituent effects on asymmetry is indicated by the systematic effects on the methyl shifts upon esterification of the propionic acid side chains. While the free acid side chains exert an influence very similar to that of ethyl groups, esterification causes them to be more electron withdrawing.[50] In E_2DC, for example, 1,3-CH_3 is slightly upfield of 5,8-CH_3 in the free acid, which reverse their relative positions upon esterification. In fact, the systematic effect on individual methyl shifts in all 2,4-R_2DC is to decrease the methyl shift asymmetry for each complex upon esterification of the propionic acid chains. Since the esterified groups are more electron withdrawing, they partially cancel the asymmetry induced by the more strongly electron-withdrawing 2,4-R_2. Since 2,4-R_2 is not electron withdrawing in E_2DC, the 5,8-CH_3 actually turn out to the upfield of 1,3-CH_3. Therefore, in a complicated low-spin ferric system, such as the protein, with possibly multiple peripheral perturbations, the observed asymmetry may be expected to reflect the *net sum of the individual perturbations.*

Relevance to Protein Studies. The variation in porphyrin methyl shift spread in Tables I and II clearly demonstrates that peripheral perturbations at the 2 and/or 4 positions are capable of producing the in-plane asymmetry characteristic of porphyrins in protein environments.[3,4,8,11,51] It thus appears very likely that the large in-plane asymmetry in the proteins is also caused by the asymmetric heme-apoprotein contacts near the porphyrin periphery. This view is supported by observations that the shift asymmetry and relative positions of individual heme methyls in low-spin sperm whale myoglobin is the same in the Met-cyano and Met-imidazole complexes.[9]

The data in Table I clearly show that shift spreads or in-plane asymmetries of a magnitude comparable to those in proteins are readily attainable with electron-withdrawing substituents at both the 2 and 4 positions. However, assignment of individual methyls demonstrates that the nature of the asymmetry differs, with the 2,4-R_2DC models always having the 8-CH_3 shift largest and the 1-CH_3 shift smallest, while the protein perturbation in myoglobins[8,9] causes 5-CH_3 to be furthest downfield and 3-CH_3 to be furthest upfield. In order to mimic the protein environment we have to turn to unsymmetrically substituted (2-R ≠ 4-R′) complexes, whose shift patterns (Table II) reveal that an electron-withdrawing substituent at the 4 positions exhibits not only a shift spread comparable to the protein, but also has 5-CH_3 downfield and 3-CH_3 upfield. Hence, the protein-induced asymmetry can be reproduced by net electron withdrawal from pyrrole II. This does not necessarily imply that the protein influence is to withdraw electron density via pyrrole II, but it does suggest that the net influence can be rationalized by the contacts either removing electron density at pyrrole II or possibly by net donation of electron density at other pyrroles, since there is evidence that multiple perturbations are additive. Since the methyl shift asymmetry has been found to be essentially identical in a variety of Met-cyano myoglobins,[12] a more careful study of the electron donating or withdrawing influences of the various invariant heme pocket amino acid residues[11] (phen CD1, His E7, His FG2, and Val E11 are most prominent) may turn out to be useful.

The data in Tables I and II also show that, since the average methyl shift in models and the proteins are also similar, the protein environment must also act primarily to rearrange the porphyrin π spin density among the four pyrroles. Thus, analysis of shift changes in a protein should focus on the net pattern for *all four methyls* rather than on a single peak, and underscores the need of not only locating all four methyls but assigning them to specific methyls on the porphyrin skeleton. Hence, shift changes in the protein with conformational change or under the influence of extrinsic perturbations would be expected to occur at all heme methyls as the electron density is redistributed within the porphyrin, *even if the perturbation is highly localized.* Thus the earlier surprising conclusion that xenon and cyclopropane intercalated[8,52,53] within the heme cavity over pyrrole II influenced all methyls rather than only 3-CH_3 (close to Xe or C_3H_6) is now easily rationalized in terms of the redistribution of the net π spin density among the four pyrroles. Detailed interpretation of these protein data is in progress and will be discussed elsewhere at a later date. These results, however, indicate that it is not unreasonable to expect that in the future the shift changes within at least low-spin ferric proteins should be interpretable in terms of details of structural changes in the heme cavity.

Acknowledgments. This work was supported by grants from the National Science Foundation, CHE-75-07788, and National Institutes of Health, HL-16087 and HL-22252.

References and Notes

(1) Colorado State University.
(2) G. N. La Mar and F. A. Walker in "The Porphyrins", D. Dolphin, Ed., Academic Press, New York, N.Y., in press.
(3) K. Wüthrich, *Struct. Bonding (Berlin)*, **8**, 53–121 (1970); W. D. Phillips in "NMR of Paramagnetic Molecules", G. N. La Mar, W. DeW. Horrocks, Jr., and R. H. Holm, Ed., Academic Press, New York, N.Y., 1973, Chapter 11.
(4) J. S. Morrow and F. R. N. Gurd, *CRC Crit. Rev. Biochem.*, **3**, 221–287 (1975).
(5) R. G. Shulman, S. H. Glarum, and M. Karplus, *J. Mol. Biol.*, **57**, 93–115 (1971).
(6) R. J. Kurland, R. G. Little, D. G. Davis, and C. Ho, *Biochemistry*, **10**, 2237–2246 (1971).
(7) H. Goff and G. N. La Mar, *J. Am. Chem. Soc.*, **99**, 6599–6606 (1977).
(8) A. Mayer, S. Ogawa, R. G. Shulman, T. Yamane, J. A. S. Cavaleiro, A. M. D'A. Rocha Gonsalves, G. W. Kenner, and K. M. Smith, *J. Mol. Biol.*, **86**, 749–756 (1974).
(9) D. L. Budd, Ph.D. Dissertation, University of California, Davis, 1978.
(10) G. N. LaMar, D. L. Budd, H. Sick, and K. Gersonde, *Biochim. Biophys. Acta*, in press.
(11) E. Antonini and M. Brunori, "Hemoglobin and Myoglobin in Their Reactions with Ligands", North-Holland Publishing Co., Amsterdam, 1971, Chapter 4.
(12) K. Wüthrich, R. G. Shulman, T. Yamane, and B. J. Wyluda, *J. Biol. Chem.*, **245**, 1947–1953 (1970).
(13) J. A. S. Cavaleiro, A. M. D'A. Rocha Gonsalves, G. W. Kenner, K. M. Smith, R. G. Shulman, A. Mayer, and T. Yamane, *J. Chem. Soc., Chem. Commun.*, 392–393 (1974).
(14) B. Evans, K. M. Smith, G. N. La Mar, and D. B. Viscio, *J. Am. Chem. Soc.*, **99**, 7070–7072 (1977).
(15) Part 2: D. B. Viscio and G. N. La Mar, *J. Am. Chem. Soc.*, following paper in this issue.
(16) D. B. Viscio and G. N. La Mar, *J. Am. Chem. Soc.*, **96**, 7354–7355 (1974).
(17) Part 3: D. B. Viscio and G. N. La Mar, *J. Am. Chem. Soc.*, accompanying paper in this issue.
(18) K. M. Smith, "Porphyrins and Metalloporphyrins", K. M. Smith, Ed., Elsevier, Amsterdam, 1975, p 12; P. Hambright, *ibid.*, p 236.
(19) W. S. Caughey, W. Y. Fujimoto, and B. R. Johnson, *Biochemistry* **5**, 3830–3843 (1966).
(20) K. Wüthrich, R. G. Shulman, B. J. Wyluda, and W. S. Caughey, *Proc. Natl. Acad. Sci. U.S.A.*, **62**, 636–642 (1969).
(21) K. Wüthrich and R. Baumann, *Helv. Chim. Acta*, **57**, 336–350 (1974).
(22) W. S. Caughey, J. C. Maxwell, J. M. Thomas, D. H. O'Keefe, and W. J. Wallace, "Metal-Ligand Interactions in Organic Chemistry and Biochemistry", B. Pullman and N. Goldblum, Ed., D. Reidel Publishing Co., Dordrecht, Holland, 1977, Part 2, pp 131–152.
(23) J. P. Jesson, "NMR of Paramagnetic Molecules", G. N. La Mar, W. DeW. Horrocks, Jr., and R. H. Holm, Ed., Academic Press, New York, N.Y., 1973, Chapter 1.
(24) G. N. La Mar and F. A. Walker, *J. Am. Chem. Soc.*, **95**, 1782–1790 (1973).
(25) G. N. La Mar in ref 23, Chapter 3.
(26) M. Karplus and G. K. Fraenkel, *J. Chem. Phys.*, **35**, 1312–1323 (1961).
(27) T. J. Swift in ref 23, Chapter 2.
(28) J. E. Falk, "Porphyrins and Metalloporphyrins", Elsevier, Amsterdam, 1964, p 179.
(29) E. W. Baker, M. Ruccia, and A. H. Corwin, *Anal. Biochem.*, **8**, 512–518 (1964).
(30) H. Fischer, "Die Chemie des Pyrrols", Part II, First Half, Leipzig, 1937, p 255.
(31) W. S. Caughey, J. O. Alben, W. Y. Fujimoto, and J. L. York, *J. Org. Chem.*, **31**, 2631–2640 (1966).
(32) J. H. Fuhrhop and K. M. Smith in ref 18, p 803.
(33) F. Sparatore and D. Mauzerall, *J. Org. Chem.*, **25**, 1073–1076 (1960).
(34) G. W. Kenner, J. M. E. Quirke, and K. M. Smith, *Tetrahedron*, **32**, 2753–2756 (1976).
(35) J. A. S. Cavaleiro, A. M. D'A. Rocha Gonsalves, G. W. Kenner, and K. M. Smith, *J. Chem. Soc., Perkin Trans. 1*, 1771–1781 (1974).
(36) Reference 28, p 126.
(37) The abbreviations for the complexes studied are as follows: protoporphyrin iron(III) dicyanide, 2,4-V_2DC; mesoporphyrin iron(III) dicyanide, 2,4-E_2DC; 2,4-dibromodeuteroporphyrin iron(III) dicyanide, 2,4-B_2DC; 2,4-diacetyldeuteroporphyrin iron(III) dicyanide, 2,4-A_2DC; 2,4-diformyldeuteroporphyrin iron(III) dicyanide, 2,4-F_2DC; 2,4-dicyanodeuteroporphyrin iron(III) dicyanide, 2,4-C_2DC; 2,4-disulfonatedeuteroporphyrin iron(III) dicyanide, 2,4-S_2DC; 2-acetyldeuteroporphyrin iron(III) dicyanide, 2-ADC; 4-acetyldeuteroporphyrin iron(III) dicyanide, 4-ADC; 2-formyl-4-vinyldeuteroporphyrin iron(III) dicyanide, 2-F,4-VDC; 2-vinyl-4-formyldeuteroporphyrin iron(III) dicyanide, 2-V, 4-FDC.
(38) J. G. Brassington, R. J. P. Williams, and P. E. Wright, *J. Chem. Soc., Chem. Commun.*, 338–340 (1975).
(39) O. Warburg, F. Neglein, and E. Haas, *Biochem. Z.*, **227**, 171–183 (1930); H. Fischer and C. V. Seeman, *Hoppe-Seyler's Z. Physiol. Chem.*, **242**, 133–157 (1936).
(40) G. N. La Mar, D. L. Budd, D. B. Viscio, K. M. Smith, and K. R. Langry, *Proc. Nat. Acad. Sci. U.S.A.*, in press.
(41) J. S. Frye, T. J. Bold, and G. N. La Mar, unpublished observations.
(42) J. Pelsach, W. E. Blumberg, and A. Adler, *Ann N.Y. Acad. Sci.*, **206**, 310–327 (1973).
(43) G. N. La Mar, J. Del Gaudio, and J. S. Frye, *Biochim. Biophys. Acta*, **498**, 422–435 (1977).
(44) Actual spread in 2,4-R_2DEC is smaller than 2,4-R_2DC; thus data for R = F, C underestimates asymmetry.
(45) The meso-H asymmetry is not readily interpreted since the origin of contact shifts (σ or π) is not understood at this time.
(46) This is due to the fact that the contact and axial dipolar methyl shifts have opposite sign and the rhombic dipolar shifts are probably nonzero.
(47) W. S. Caughey, H. Eberspaecher, W. H. Fuchsman, S. McCoy, and J. O.

Alben, *Ann. N.Y. Acad. Sci.*, **153**, 722–737 (1969).
(48) W. I. White in "The Porphyrins", D. Dolphin, Ed., Academic Press, New York, N.Y., in press.
(49) The shifts for 2,4-F_2DC were obtained by correcting the 2,4-F_2DEC shifts with the esterification shifts listed in the text.
(50) H. H. Jaffe, *Chem. Rev.*, **53**, 191–261 (1953); R. W. Taft, Jr., N. C. Deno, and P. S. Skell, *Annu. Rev. Phys. Chem.*, **9**, 287–314 (1958).
(51) D. L. Budd, G. N. La Mar, and K. M. Smith, to be published.
(52) R. G. Shulman, J. Peisach, and B. J. Wyluda, *J. Mol. Biol.*, **48**, 517–523 (1970).
(53) B. P. Schoenborn, H. C. Watson, and J. C. Kendrew, *Nature (London)*, **207**, 28–30 (1965).

NMR Studies of Low-Spin Ferric Complexes of Natural Porphyrin Derivatives. 2. Determination of the Dimer Structure of the Biscyano Complex Using Intermolecular Paramagnetic Dipolar Relaxations

David B. Viscio and Gerd N. La Mar*

Contribution from the Department of Chemistry, University of California, Davis, California 95616. *Received May 30, 1978*

Abstract: The ^{1}H NMR spectra of 2,4-dibromodeuteroporphinatoiron(III) dicyanide recorded below −40 °C exhibit significant concentration-dependent line widths and longitudinal relaxation rates. These intermolecular paramagnetic dipolar relaxation rates are highly regioselective and permit determination of the solution structure of the dimer which consists of the overlap of a single pyrrole from each porphyrin. The contact is highly stereospecific, involving the overlap of pyrrole I of one porphyrin with pyrrole IV of the other porphyrin complex within the dimer. The ≤4 Å spacing between essentially parallel porphyrin planes is consistent with a π–π complex. Since the π contact in the dimer involves the pyrroles suggested to be the best π acceptor (I) and best π donor (IV) based on spin density asymmetry, donor/acceptor π–π interactions are proposed as contributing to the dimer stability.

Introduction

The dimerization of metalloporphyrins in solution is a well-documented phenomenon[1] whose study has been pursued, in part, in order to gain insight into the unusual properties of the large polarizable π-electron systems. The characterization of the dimer structures in solution has relied primarily on the analysis of intermolecular ^{1}H NMR ring current shifts in the case of diamagnetic porphyrins,[2] and intermolecular electron-spin dipolar interactions in paramagnetic complexes.[3] We wish to demonstrate here that intermolecular paramagnetic dipolar relaxation[4,5] can also be profitably utilized for structure analysis, and that this method is particularly well suited for probing highly stereospecific interactions between porphyrins within a dimer.

Although the ^{1}H NMR spectra of the 2,4-substituted deuteroporphyrin iron(III) dicyanide complexes[6] ($S = 1/2$) were found to be concentration independent in methanol at ambient temperatures,[7] spectra recorded below −40 °C exhibited significant concentration-dependent line positions as well as line widths. Computer analysis of the concentration-dependent shifts was shown to be consistent with an equilibrium involving solely monomer and dimer,[8] and equilibrium constants in the range 5–50 L mol^{-1} were found for various R, with 2,4-dibromodeuteroporphyrin iron(III) dicyanide exhibiting the largest degree of dimerization.

Solution ESR of these low-spin ferric complexes cannot be resolved,[9] and analysis of the concentration-dependent NMR shifts is not possible because the dimer shifts arise from the sum of intermolecular positive ring-current shifts and negative paramagnetic dipolar shifts which cannot be readily separated.

The observed stereospecific intermolecular relaxation, however, is due exclusively to paramagnetic dipolar relaxation (vide infra) caused by the second iron atom in the dimer. This intermolecular relaxation contribution is proportional to r_1^{-6}, the distance to the second iron atom, and should be of utility in elucidating the structure of the dimer. A preliminary report[5] on the qualitative structure determination of the dimer of protoporphyrin iron(III) dicyanide in $C^2H_3O^2H$ has already been presented. We will explore here the utility of intermolecular dipolar T_1 relaxation as a tool for determining the solution dimer structure of 2,4-dibromodeuteroporphyrin iron(III) dicyanide.

The qualitative aspects of the observed stereospecific intermolecular relaxation are found to be the same in all complexes with electron-withdrawing substituents at the 2,4 position.[7,8] The dibromo complex was chosen for detailed study because its thermodynamics of dimerization could be characterized most readily,[8] its proton spectrum is the best resolved in the critical methyl region,[7] permitting accurate T_1 determinations, and the absence of protons in the 2,4 substituents permits the resolution of all nonequivalent protons in the complex over the widest range of temperature and concentration.

In addition to assessing the use of intermolecular dipolar relaxation as a solution structure tool for porphyrin dimers, we are interested in determining if the major interaction between the porphyrins involves the contact of the two π systems suggestive of π–π donor–acceptor interaction,[10] and whether the asymmetry characterized by the spread of the methyl contact shifts, as discussed in part 1 of this study,[7] plays a major role in controlling the stereospecificity of the π contacts.

Principles

The observation of concentration-dependent relaxation rates will yield data which can be used to determine relaxation rates in the pure dimer. For the system in rapid exchange on the NMR time scale (only one set of resonances was observed) between the monomer and dimer, the observed relaxation rates,

0002-7863/78/1500-8092$01.00/0